## PAPER

# An electron poor iridium pincer complex for catalytic alkane dehydrogenation†

Oleksandr O. Kovalenko and Ola F. Wendt*

A novel electron deficient 4,6-bis(trifluoromethyl)-1,3-phenylene diphosphinite ligand **4** was developed and synthesized. Reaction of Ir precursors with ligand **4** gave chloro(hydride) pincer complex **5**, which demonstrated a higher TON in alkane dehydrogenation reactions compared to similar phosphinite based pre-catalysts. The formation of cyclooctene (COE) and *tert*-butylethylene adducts of the 14e catalysts was also studied and the COE adduct is implicated as the resting state of the catalyst. All compounds were characterized by NMR spectroscopy and, in addition, the molecular structures of key complexes were confirmed by X-ray analysis.

## Introduction

The selective functionalization of alkanes is a challenging topic in modern organic chemistry.[1] One highly demanded reaction, particularly in industry, is the conversion of inert alkanes into more reactive olefins, which opens up broad possibilities for further transformations and modifications. In fact, olefins are the most important starting material for making industrial organic chemicals. Industrial catalytic alkane dehydrogenations proceed at high temperatures (*ca.* 400–600 °C),[2] and effective homogeneous alkane dehydrogenation catalysts operating under relatively low temperature conditions are therefore highly desirable.

The first homogeneous alkane dehydrogenation catalytic systems were described in the 1980s by Crabtree and Felkin.[3] The temperature of the catalytic process was decreased down to 150 °C, but the turnover numbers (TONs) were rather low due to catalyst decomposition. The results reported by Kaska and Jensen using a very robust and efficient iridium hydrido complex (**I**) opened up a new pincer era in catalytic alkane dehydrogenation research (Fig. 1).[4]

Many variations of the pincer framework have been explored including both aromatic and aliphatic backbones and the highest TONs were reported for aromatic backbones with oxygen and/or sulfur linkers on the arm.[5–9] Thus, bis-phosphinite complex **II** demonstrates a significantly higher TON in alkane transfer dehydrogenation compared to complex **I**
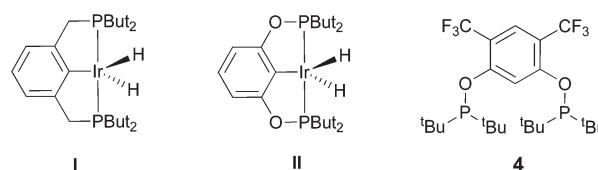


**Fig. 1** Previously reported pincer-iridium catalysts **I–II** and the herein developed ligand **4** for catalytic alkane dehydrogenation.

(Fig. 1). Furthermore, the electron withdrawing substituents in the aromatic ring increase the catalyst performance.[6]

Based on these findings, we decided to investigate a bis-phosphinite aryl backbone with two strong electron withdrawing CF$_3$ groups in the *meta*-position with respect to the metallation site. This should give maximum inductive, electronic communication with the metal and, in addition, undesired orthometallated byproduct formation should be avoided.[10] Thus, we herein report the synthesis of electron poor ligand **4** and its metallation to afford the corresponding iridium pincer complex. The reactivity of this complex and its catalytic activity in alkane dehydrogenation are described.

## Experimental section

### General information

All manipulations were carried out under a dry Ar or N$_2$ atmosphere using standard Schlenk or glovebox techniques, unless otherwise noted. All catalytic experiments were performed under a dry Ar atmosphere. Hydrocarbon solvents were degassed and distilled from sodium benzophenone ketyl prior to use. Chlorinated solvents were degassed and distilled from CaH$_2$. Silica gel with 60 Å pore size and 230–400 mesh was

*Centre for Analysis and Synthesis, Department of Chemistry, Lund University, P. O. Box 124, S-221 00 Lund, Sweden. E-mail: ola.wendt@chem.lu.se*

used for column chromatography. All other solvents, reagents and chemicals were used as received.

^{1}H, ^{19}F, ^{31}P, and ^{13}C NMR spectra were recorded at 400, 376, 162 and 100 MHz, respectively, using a Bruker 400 MHz spectrometer. For compounds **1–3** chloroform-d and for compounds **4–9** benzene-$d_6$ were used and chemical shifts were referenced to the residual solvent peaks.[11] Elemental analysis was performed by H. Kolbe Microanalytisches Laboratorium, Mülheim an der Ruhr, Germany. High-resolution mass spectra (HRMS) were recorded on a Waters Xevo Q-TOF mass spectrometer using electrospray ionization and lock mass corrections.

### Crystallography

The crystallographic measurements were performed at 293 K using an Oxford Diffraction Xcalibur 3 system with Mo-Kα radiation.[12] Data collection, cell refinement, and data reduction and analysis were carried out using the Xcalibur PX software, CRYSALIS CCD and CRYSALIS RED.[13] Analytical absorption corrections were applied to the data using CRYSALIS RED. All structures were solved by direct methods using SHELXS-2014 and refined by a full-matrix least-squares technique based on $F^2$ using SHELXL-2014 with anisotropic thermal parameters for all non-H atoms.[14] Hydrogen atoms were constrained to parent sites, using a riding model.

### Preparations

**1,3-Dibromo-4,6-bis(trifluoromethyl)benzene (1).** Compound **1** was prepared according to a previously reported procedure.[15] 15.07 g of bis(trifluoromethyl)aniline were used to give 7.75 g (32%) of **1** as a pink solid.

^{1}H NMR (CDCl_3, 400 MHz): $\delta$ 8.12 (s, 1H), 7.95 (s, 1H); ^{19}F NMR (CDCl_3, 376 MHz): $\delta$ −63.07 (s); ^{13}C NMR (CDCl_3, 100 MHz): $\delta$ 140.87, 129.84 (q, $J$ = 33.0 Hz), 126.80 (sep, $J$ = 5.5 Hz), 124.76, 122.05 (q, $J$ = 273.0 Hz).

**4,6-Bis(trifluoromethyl)resorcinol dibenzyl ether (2).** In a 150 mL Schlenk flask, benzyl alcohol (2.59 mL, 25.01 mmol) was added dropwise to a suspension of KH (25.53 mmol, 1.02 g) in dry THF (40 mL) at r.t. and the reaction mixture was stirred for 4 h at 40 °C. 0.29 g (2.01 mmol) of CuBr and 3.72 g (10.00 mmol) of **1** were added portion-wise and the mixture was refluxed for 12 h. The solvent was evaporated, and the residue was quenched with a saturated solution of NH_4Cl in water and extracted with DCM (4 × 50 mL). The combined organic layers were washed with brine and dried over Na_2SO_4 and the solvent was evaporated. The crude product was purified by column chromatography using pentane/DCM as an eluent, affording 3.75 g (88%) of the target compound **2** as a white solid.

^{1}H NMR (CDCl_3, 400 MHz): $\delta$ 7.81 (s, 1H), 7.46–7.32 (m, 10H), 6.61 (s, 1H), 5.16 (s, 4H); ^{19}F NMR (CDCl_3, 376 MHz): $\delta$ −61.55 (s); ^{13}C NMR (CDCl_3, 100 MHz): $\delta$ 160.38, 135.33, 128.86, 128.39, 126.78, 126.54 (sep, $J$ = 5.5 Hz), 123.27 (q, $J$ = 269.7 Hz), 111.14 (q, $J$ = 32.0 Hz), 99.26, 70.70. HRMS (ESI, $m/z$) calcd for $C_{22}H_{15}O_2F_6$ [M − H^{+}]: 425.0976; found: 425.0976.

**4,6-Bis(trifluoromethyl)resorcinol (3).** In a 1 L round-bottom flask, 0.38 g of Pd/C (10 wt%) was added to a solution of **2** (3.75 g, 8.80 mmol) in MeOH (400 mL). The reaction mixture was stirred overnight under a H_2 atmosphere at r.t. The Pd/C was filtered off and the solvent was evaporated. The crude product was purified by vacuum sublimation at 50 °C and 40 mmHg. Yield: 2.04 g, 94% of a white crystalline compound. ^{1}H NMR (CDCl_3, 400 MHz): $\delta$ 7.68 (s, 1H), 6.55 (s, 1H), 5.74 (s, 2H); ^{19}F NMR (CDCl_3, 376 MHz): $\delta$ −59.95 (s); ^{13}C NMR (CDCl_3, 100 MHz): $\delta$ 157.68, 126.59 (sep, $J$ = 5.0 Hz), 123.51 (q, $J$ = 270.0 Hz), 109.67 (q, $J$ = 32.0 Hz), 106.54. HRMS (ESI, $m/z$) calcd for $C_8H_3O_2F_6$ [M − H^{+}]: 245.0033; found: 245.0037.

**((4,6-Bis(trifluoromethyl)-1,3-phenylene)bis(oxy))bis(di-*tert*-butylphosphine) (4).** In a Schlenk flask, KH (0.060 g, 1.49 mmol) was added to a solution of **3** (0.350 g, 1.42 mmol) in THF (10 mL) and the mixture was stirred for 4 h at 40 °C. Di-*tert*-butylchlorophosphine (0.283 mL, 1.49 mmol) was added dropwise and the mixture was stirred overnight at room temperature. Then, the procedure was repeated with new KH (0.060 g, 1.49 mmol) and di-*tert*-butylchlorophosphine (0.289 mL, 1.52 mmol). Finally, all volatiles were evaporated, 3 mL of dry benzene was added and the precipitate was filtered off. Removal of the solvent *in vacuo* yielded a yellow solid, which was dissolved in 3 ml of pentane. The solution was cooled down to −21 °C in order to induce crystallization. Yield: 0.395 g (52%) of white crystals. ^{1}H NMR (C_6D_6, 400 MHz): $\delta$ 8.42 (t, $J$ = 8.0 Hz, 1H), 7.84 (s, 1H), 1.08 (d, $J$ = 12.0 Hz, 36H); ^{19}F NMR (C_6D_6, 376 MHz): $\delta$ −60.49 (s); ^{31}P NMR (C_6D_6, 162 MHz): $\delta$ 156.05 (m); ^{13}C NMR (C_6D_6, 100 MHz): $\delta$ 161.60 (d, $J$ = 11.0 Hz), 126.63 (sep, $J$ = 5.0 Hz), 123.81 (q, $J$ = 269.5 Hz), 111.85 (q, $J$ = 31.0 Hz), 106.90 (t, $J$ = 27.5 Hz), 35.71 (d, $J$ = 27.0 Hz), 26.81 (d, $J$ = 16.0 Hz).

**CF_3(POCOP)IrHCl (5). Method A.** In a thick wall Straus flask, compound **4** (0.104 g, 0.195 mmol) and cyclooctadiene iridium chlorido dimer [Ir(μ[2]-Cl)(COD)]_2 (0.065 g, 0.097 mmol) were combined in toluene. The reaction vessel was sealed, placed in an oil bath and stirred overnight at 120 °C. The toluene was removed under vacuum and the dark brown residue was purified by column chromatography gradually changing the eluent from hexane (100%) to hexane : DCM (2 : 1). Removal of the solvent gave 0.096 g, 65% of a red solid. Deep red crystals suitable for X-ray analysis were obtained by slow evaporation of the hexane solution under an argon atmosphere.

**Method B.** In a thick wall Straus flask, compound **4** (0.214 g, 0.400 mmol) and chlorobis(cyclooctene)iridium dimer [Ir(μ[2]-Cl)(COE)_2]_2 (0.179 g, 0.200 mmol) were combined in benzene. The reaction vessel was sealed, placed in an oil bath and stirred overnight at 90 °C. The solvent was removed under vacuum and the dark brown residue was purified by column chromatography gradually changing the eluent from hexane (100%) to hexane : DCM (2 : 1). Removal of the solvent gave 0.261 g, 86% of a red solid. ^{1}H NMR (C_6D_6, 400 MHz): $\delta$ 7.57 (s, 1H), 1.20 (vt, $J$ = 15.0 Hz, 18H), 1.15 (vt, $J$ = 15.0 Hz, 18H), −40.44 (t, $J$ = 14.0 Hz, 1H); ^{19}F NMR (C_6D_6, 376 MHz,): $\delta$ −61.74 (s); ^{31}P NMR (C_6D_6, 162 MHz): $\delta$ 184.73 (m); ^{13}C NMR

($C_6D_6$, 100 MHz): $\delta$ 165.88 (vt, $J$ = 12.0 Hz), 124.15 (t, $J$ = 3.0 Hz), 123.63 (q, $J$ = 270.0 Hz), 120.79 (sep, $J$ = 5.0 Hz), 108.35 (qvt, $J$ = 32.3 Hz, $J$ = 9.6 Hz), 43.02 (vt, $J$ = 22.0 Hz), 39.50 (vt, $J$ = 22.0 Hz), 26.90 (vt, $J$ = 6.6 Hz). Anal. Calcd for $C_{24}H_{38}O_2P_2IrClF_6$: C, 37.82; H, 5.03. Found C, 38.22, H, 5.22.

**$^tBu_2P(OH)(COD)IrCl$ (6).** Compound **6** was obtained as a byproduct using method A for the synthesis of complex **5** and purified by column chromatography using hexane : DCM (9 : 1) as the eluent. Yield: 9 mg, 9% of pale red solid. Single crystals suitable for X-ray analysis were obtained by recrystallization from pentane. Spectroscopic data of compound **6** were reported previously by Buono and coworkers.[16]

**$CF_3(POCOP)Ir(L)$ (7).** Complex **5** (0.0100 g, 0.0131 mmol) and $^tBuONa$ (0.0014 g, 0.0144 mmol) were placed in a Straus flask. Degassed dry benzene (0.6 mL) was distilled into the reaction vessel, and the mixture was stirred overnight at room temperature and then filtered through a PTFE filter (0.2 µm). Removal of volatiles *in vacuo* yielded an orange solid. $^1H$ NMR ($C_6D_6$, 400 MHz): $\delta$ 7.70 (s, 1H), 1.01 (vt, $J$ = 15.0 Hz, 36H); $^{19}F$ NMR ($C_6D_6$, 376 MHz,): $\delta$ −61.45 (s); $^{31}P$ NMR ($C_6D_6$, 162 MHz): $\delta$ 188.64 (m). $^{13}C$ NMR ($C_6D_6$, 100 MHz): $\delta$ 166.41 (vt, $J$ = 13.2 Hz), 149.97 (t, $J$ = 5.0 Hz), 124.37 (q, $J$ = 271.4 Hz), 122.06 (sep, $J$ = 5.0 Hz), 107.75 (qvt, $J$ = 32.2 Hz, $J$ = 10.2 Hz), 40.39 (vt, $J$ = 23.4 Hz), 27.22 (vt, $J$ = 5.1 Hz).

**$CF_3(POCOP)Ir(COE)$ (8).** 0.018 mL (0.140 mmol) of degassed dry COE was added to a 0.500 mL benzene solution of **7** (0.010, 0.014 mmol) in a J. Young NMR tube. All volatiles were evaporated and 0.510 mL of degassed dry deuterated benzene was added. This resulted in a deep red solution which was analyzed by NMR spectroscopy. Deep red crystals suitable for X-ray analysis were obtained by slow evaporation of benzene under an argon atmosphere. $^1H$ NMR ($C_6D_6$, 400 MHz): $\delta$ 7.79 (s, 1H), 4.58–4.48 (m, 2H), 2.55–2.45 (m, 2H), 2.05–1.95 (m, 2H), 1.68–1.57 (m, 4H), 1.48–1.33 (m, 4H), 1.27 (vt, $J$ = 14.0 Hz, 36H); $^{19}F$ NMR ($C_6D_6$, 376 MHz,): $\delta$ −61.04 (s); $^{31}P$ NMR ($C_6D_6$, 162 MHz): $\delta$ 185.48 (br s); $^{13}C$ NMR ($C_6D_6$, 100 MHz): $\delta$ 167.02 (vt, $J$ = 12.0 Hz), 146.62 (t, $J$ = 6.7 Hz), 124.35 (q, $J$ = 268.0 Hz), 122.89 (sep, $J$ = 5.0 Hz), 106.41 (qvt, $J$ = 32.6 Hz, $J$ = 10.4 Hz), 64.71, 41.75 (vt, $J$ = 19.2 Hz), 33.98, 32.72, 28.70 (vt, $J$ = 5.8 Hz), 26.42.

### General procedure for the catalytic dehydrogenation of COA with TBE

Complex **5** (0.0030 g, 0.0040 mmol, 1.0 eq.), $^tBuONa$ (0.0006 g, 0.0060 mmol, 1.5 eq.), degassed dry cyclooctane (COA) (1.631 mL, 12.12 mmol, 3030 eq.) and *tert*-butylethylene (TBE) (1.562 mL, 12.12 mmol, 3030 eq.) were placed in a Straus flask. The flask was sealed and fully immersed into a pre-heated oil bath with the specified temperature and time. Thereafter, the flask was cooled down in an ice bath and the sample was analyzed by NMR spectroscopy. Three runs were performed to determine the average TONs. No compounds other than COA, cyclooctene (COE), cyclooctadiene (COD), TBE and *tert*-butylethane (TBA) could be detected by $^1H$ NMR spectroscopy. This procedure was used also for other iridium complexes.

## Results and discussion

### Synthesis and characterization of ligands and complexes

Ligand **4** was synthesized in five steps following the strategy described in Scheme 1, starting from bis(trifluoromethyl) aniline. Compound **1** was obtained in 32% yield following a previously described procedure of Williams *et al.*[15] All attempts to obtain key resorcinol **3** in one step from **1** using either tetrabutylammonium hydroxide or alkali metal hydroxide media following reported catalytic protocols were unsuccessful, probably due to the electron poor nature of structure **1** and the necessity to substitute two bromine atoms at the same time.[17] Instead, the synthesis of benzyl ester **2** was performed using an Ullmann-type reaction with CuBr as the catalyst.[18] Thus, the target ligand **4** was obtained in 14% total yield and fully characterized by $^{31}P$, $^{19}F$, $^{13}C$ and $^1H$ NMR spectroscopy. Its structure was confirmed with a single crystal X-ray analysis and the molecular structure is given in Fig. 2. This shows that the trifluoromethyl groups cause substantial steric hindrance, obstructing the free rotation of the phosphinite groups across the C–O bond. Hence, the arms of the pincer ligand are oriented in the same direction, possibly providing some assistance in the cyclometallation reactions.
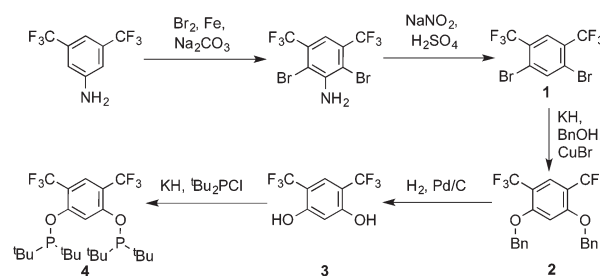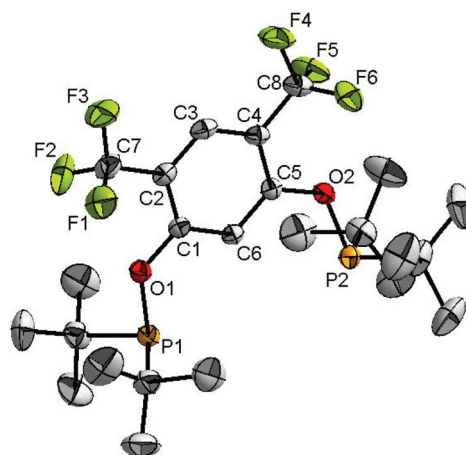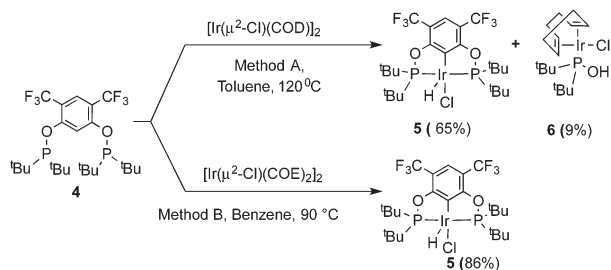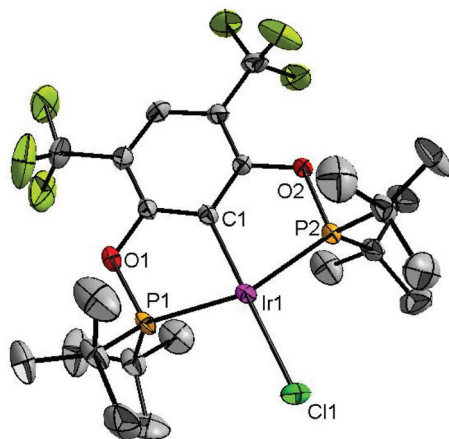


**Scheme 1** Synthesis of ligand **4**.



**Fig. 2** The molecular structure of compound **4**. Thermal ellipsoids are drawn at the 30% probability level. Hydrogen atoms are omitted for clarity. Selected bond lengths (Å) and angles (°): C1–O1 1.359(3), O1–P1 1.6915(18), C5–O2 1.360(3), O2–P2 1.6937(18), C1–O1–P1 122.83(15), C5–O2–P2 122.80(15).

The reaction progress of the cyclometallation of ligand **4** with iridium precursors could be conveniently monitored by $^{31}P\{^1H\}$ and/or $^{19}F\{^1H\}$ NMR spectroscopy. After stirring **4** with the cyclooctadiene iridium chloride dimer $[Ir(\mu^2\text{-}Cl)(COD)]_2$ in toluene at room temperature for one hour, an orange precipitate was formed and no signal could be observed in the $^{31}P\{^1H\}$ NMR spectrum. This behaviour is typical in the formation of non-cyclometallated dimers, which usually have very low solubility.[19] However, in this case the dimer could be transformed further; heating the reaction mixture at 120 °C dissolved the precipitate, forming a deep red solution. There was a concomitant appearance of new signals at 184.73 ppm and −61.74 ppm in the $^{31}P\{^1H\}$ and $^{19}F\{^1H\}$ NMR spectra, correspondingly. From this reaction the iridium hydrido chloride complex, **5**, was obtained in 65% yield (*cf.* Scheme 2). The $^1H$ NMR spectrum of **5** displays the characteristic hydride triplet at −40.44 ppm,[6b] and the molecular structure was also confirmed using X-ray crystallography (Fig. 3). As seen from the figure, the iridium atom displays a distorted square-pyramidal geometry assuming that the hydride is in an axial position. The complex has the usual P–Ir–P angle of less than 180° and the Ir–P bond lengths are very similar. The electron withdrawing nature of the ligand is displayed in the unusually short Ir–Cl distance of 2.384(2) Å, which is *ca.* 0.01 Å shorter than the corresponding unsubstituted one (Table 1).[19b]

In addition to the main product **5**, complex **6** was isolated as a byproduct in 9% yield (Scheme 2). We could establish the molecular structure of **6** using single crystal X-ray analysis; the molecular structure is given in Fig. 4. This compound was previously synthesized and characterized by Buono and co-workers,[16] but in our hands it crystallizes in a higher symmetry space group, $P2_1/n$. From the structure it is evident that iridium cleaved the C–O bond in one of the pincer phosphinite arms, forming a di(*tert*-butyl)phosphinous acid iridium complex with a distorted square planar geometry. Such a C–O bond cleavage in pincer complexes has been observed previously.[20]

**Scheme 2** Synthesis of complex **5**.

**Fig. 3** The molecular structure of complex **5**. Thermal ellipsoids are drawn at the 30% probability level. Hydrogen atoms are omitted for clarity. Selected bond lengths (Å) and angles (°): Ir1−C1 1.997(5), Ir1−P1 2.2946(15), Ir1−P2 2.2919(15), Ir1−Cl1 2.3840(16), P1−Ir1−P2 160.59(5), C1−Ir1−Cl1 174.67(15).

### Dehydrogenation catalysis

In order to investigate the catalytic activity in alkane transfer dehydrogenation reactions, we chose a common benchmark reaction – transfer dehydrogenation of cyclooctane in the presence of *tert*-butylethylene (TBE). The standard conditions and COA/TBE/catalyst ratio (3030/3030/1) were used in the initial catalytic studies, which gave us the possibility to compare catalyst **5** with previously reported ones.[6,7] To generate an active catalyst, $^t$BuONa (1.5 eq.) was added in order to remove HCl from **5**. This formed a compound, **7**, which could be isolated as an orange solid and characterized by $^{31}P$, $^{19}F$, $^{13}C$ and $^1H$ NMR spectroscopy. The $^{31}P$ and $^{19}F\{^1H\}$ NMR spectra contain signals at 188.64 ppm and a sharp singlet at −61.45 ppm, respectively. Furthermore, the $^1H$ NMR spectrum only contains signals from the ligand with no indication of any dynamic behaviour as previously observed for more electron rich pincer systems.[22] It seems unlikely that **7** is a 14e complex and we tentatively

**Table 1** Select bond lengths (Å) for electron-rich and -deficient pincer phosphinite complexes.[6b,19b,21,25b]

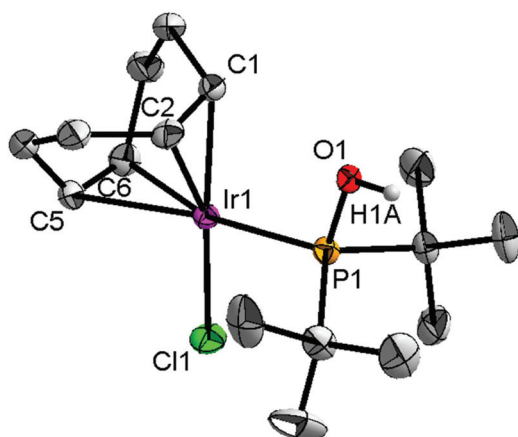| | 5 | ref.[20] | ref.[19b] | ref.[20] | ref.[6b] | ref.[25b] |
|---|---|---|---|---|---|---|
| Ir–Cl | 2.3840(16) | 2.3933(13) | 2.3947(12) | 2.3954(8) | 2.4044(14) | 2.4115(12) |
| Ir–C(1) | 1.997(5) | 1.992(4) | 2.000(3) | 1.996(3) | 2.004(5) | 2.014(4) |
| Ir–P(1) | 2.2946(15) | 2.2871(13) | 2.2897(10) | 2.2890(8) | 2.2949(16) | 2.2944(12) |
| Ir–P(2) | 2.2919(15) | 2.2864(13) | 2.2925(11) | 2.2940(8) | 2.2889(15) | 2.2926(11) |

**Fig. 4** The molecular structure of complex **6**. Thermal ellipsoids are drawn at the 30% probability level. Hydrogen atoms are omitted for clarity. Selected bond lengths (Å) and angles (°): Ir1–C1 2.125(5), Ir1–C2 2.117(5), Ir1–C5 2.228(5), Ir1–C6 2.217(5), Ir1–Cl1 2.3573(13), Ir1–P1 2.2728(13), P1–O1 1.593(3), P1–Ir1–Cl1 94.74(5), Ir1–P1–O1 110.76(13).

describe it as the benzene adduct. The electron poor ligand in **7** probably prohibits dynamic oxidative addition/reductive elimination of benzene (see the ESI†). However, it is likely that there is a fast benzene exchange at the metal centre (without oxidative addition). Attempts to characterize **7** with elemental analysis failed since it quickly forms a dinitrogen complex.

After heating the reaction vessel for 24 h at 200 °C, complex **7** demonstrated a turnover number (TON) of 2086. This value is higher than the original Brookhart's catalyst with an unsubstituted benzene ring and also slightly higher than values obtained using other electron withdrawing substituents (Table 3).[6,8] A temperature screening was performed and an improved performance of **7** was detected at 170 °C (Table 2); thus, this temperature was used for the following experiments. A kinetic study showed that around 80% of the turnovers were observed within the first 8 hours of the reaction and ≈90% after 24 h. Prolonged heating did not improve turnovers substantially (Table 4 and Fig. 5). An initial TOF could be calculated and it was around 0.8 s$^{-1}$, which is lower than that reported for $\{p\text{-}C_6F_5\text{-}C_6H_2(OCH_2P^tBu_2)_2\}$Ir, but on the other hand our experiment was performed at a 30 °C lower temperature. For a direct comparison the same experiment was

**Table 2** Temperature screening in transfer dehydrogenation of COA with TBE catalyzed by *in situ*-generated complex **7**

| $t$ [°C][a] | TONs[b] |
| --- | --- |
| 150 | 1551 |
| 160 | 2276 |
| 170 | 2324 |
| 180 | 2109 |
| 200 | 2086 |

[a] Average of three runs, using a 3030 : 3030 : 1 ratio of COA/TBE/precatalyst **5** and 1.5 equiv. of $^t$BuONa for 24 h. [b] Determined by $^1$H NMR, the sum of COE and COD double bonds equals the TON of TBE within 2% difference.

**Table 3** Various iridium phosphinite catalysts in the catalytic dehydrogenation of COA[6,8]



| Complex | TONs[a] |
| --- | --- |
| **5** | 2398[b] |
| | 2086[c] |
| | 2070[d] |
| C$_6$F$_5$-Cat | 2041[d] |
| F-Cat | 1530[d] |
| H-Cat | 1583[d] |

[a] Results were obtained using a 3030 : 3030 : 1 ratio of COA/TBE/precatalyst and $^t$BuON under an argon atmosphere. TONs were determined by $^1$H NMR. [b] Obtained at 170 °C for 40 h. [c] Obtained at 200 °C for 24 h. [d] Obtained at 200 °C for 40 h.

**Table 4** Catalytic activity of *in situ*-generated complex **7** in the transfer dehydrogenation of COA with TBE



| Entry[a] | $t$ [h] | TONs[b] | Entry[a] | $t$ [h] | TONs[b] |
| --- | --- | --- | --- | --- | --- |
| 1 | 0.17 | 625 | 7 | 8 | 1985 |
| 2 | 0.5 | 1117 | 8 | 15 | 2174 |
| 3 | 1 | 1382 | 9 | 24 | 2324 |
| 4 | 3 | 1781 | 10 | 40 | 2398 |
| 5 | 4 | 1851 | 11 | 170 | 2537 |
| 6 | 6 | 1935 | 12[c] | 24 | 10 |

[a] Average of three runs, using a 3030 : 3030 : 1 ratio of COA/TBE/precatalyst **5** and 1.5 equiv. of $^t$BuONa, unless otherwise noted. All reactions were performed under an argon atmosphere. [b] Determined by $^1$H NMR, the sum of COE and COD double bonds equals the TON of TBE within 2% difference. [c] Using a 3030 : 1 ratio of COA/precatalyst **5** and 1.5 equiv. of $^t$BuONa under argon under refluxing conditions.

performed with the Brookhart catalyst (**II**), reproducing the literature results fairly well (Table S2† and Fig. 5). It again shows that the initial TOF of **5** is lower (at a lower temperature) but the TON is higher.

Also, catalysis without a hydrogen acceptor (TBE) was investigated. This was conducted in an open vessel protected with an argon backstop. This approach provides unimpeded hydrogen elimination from the reaction flask, but puts limits on the maximum reaction temperature because of the boiling point of COA and COE (max. $t \approx 150$ °C). Under these conditions we only observed *ca*. 10 turnovers after 24 h (Table 4).
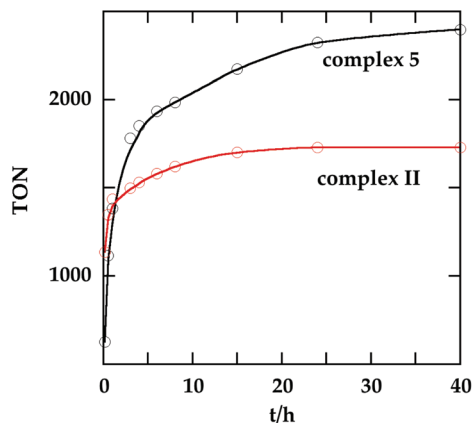
**Fig. 5** Turnover number as a function of time for **5** (at 170 °C) and **II** (at 200 °C). The final TON of **II** is 1730. See Tables 4 and S2† for details.



**Fig. 6** The molecular structure of complex **8**. Thermal ellipsoids are drawn at the 30% probability level. Hydrogen atoms are omitted for clarity. Selected bond lengths (Å) and angles (°): Ir1–C1 2.032(9), Ir1–P1 2.285(5), Ir1–P2 2.315(5), Ir1–C25 2.289(12), Ir1–C26 2.230(12), C25–C26 1.380(18), P1–Ir1–P2 157.15(10), C1–Ir1–C25 159.4(5), C1–Ir1–C26 160.2(7).

## Isolation of intermediates

To probe the resting state of the catalyst the reaction mixture after catalysis was analyzed by $^{31}P\{^{1}H\}$ NMR spectroscopy. The presence of a dominant broad signal at 185.48 ppm was observed, which triggered us to examine the nature of the contributing species. Previous mechanistic studies[23] have shown that the resting state varies with the electronic nature of the catalyst, with the lower oxidation states being favoured for more electron poor systems.[24]

Compound **7** reacts with COE and TBE in benzene solution at room temperature forming deep red solutions of complexes **8** and **9**, correspondingly (Scheme 3). $^{31}P$ and $^{19}F\{^{1}H\}$ NMR spectra demonstrate chemical shifts at 185.48 ppm, 185.45 ppm, −61.04 ppm and −61.47 ppm, respectively. The signal from **8** agrees very well with the signal of the reaction mixture after catalysis. Evaporation of volatile TBE and benzene from the solution of **9** led to the formation of compound **7** again, and **9** could not be isolated in a pure form. Contrary to **9**, complex **8** did not lose coordinated COE readily, and based on $^{31}P$, $^{19}F$, $^{13}C$ and $^{1}H$ NMR studies of the deuterated benzene solutions an equilibrium was established between complex **8**, precursor **7** and free COE in a ratio of 2 : 1 : 1. Compound **8** is poorly soluble in benzene, and X-ray quality crystals were obtained and an X-ray analysis was performed to confirm the molecular structure of **8**, which is given
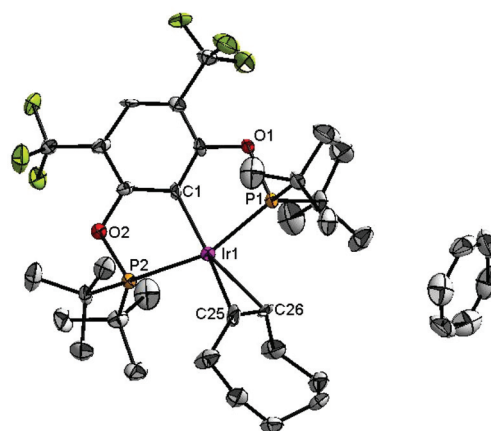
in Fig. 6. The structure exhibits a distorted square planar geometry with the olefin bonded perpendicular to the coordination plane. Bond lengths and angles are in good agreement with similar, previously reported complexes with coordinated ethylene and COE. The C=C bond is 1.380(18) indicating a fairly weak back-donation from the Ir(ı) metal centre.[25,26]

These experiments show that COE binds much more strongly than TBE to compound **7**. As the COE concentration rises, the activity consequently decreases and already at moderate COE concentrations, **8** is probably the resting state of the catalyst. In keeping with the electron poorness of the ligand system there is no oxidative addition observed. As mentioned previously, **7** does not seem to undergo oxidative addition of benzene and the olefin substrates show no tendency for any vinylic C–H oxidative addition; the oxidative addition of COA is therefore probably the rate determining step in the catalytic dehydrogenation.

## Conclusions

A new electron deficient ligand **4** was synthesized and the iridium precatalyst **5** was successfully obtained and characterized. With a base, this gives the active species **7**, which could be isolated probably as the benzene adduct. The catalyst demonstrated an increase in the TON compared to other iridium phosphinite systems. Also, a relatively stable COE complex **8** was obtained and characterized. This compound is probably the resting state of the catalyst already at low conversion.

## Acknowledgements
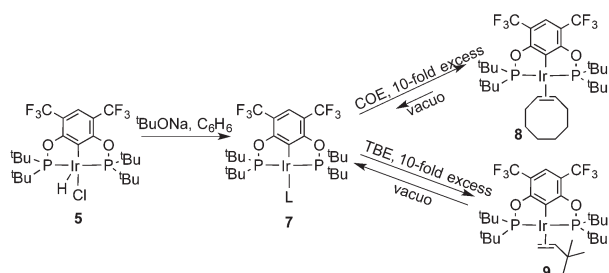
**Scheme 3** Reactions of complex **5** with TBE and COE.

# References

1 (a) J. F. Hartwig, *J. Am. Chem. Soc.*, 2016, **138**, 2–24; (b) J. A. Labinger and J. E. Bercaw, *Nature*, 2002, **417**, 507–514; (c) K. M. Waltz and J. F. Hartwig, *Science*, 1997, **277**, 211–213.

2 K. Weissermel and H.-J. Arpel, *Industrial Organic Chemistry*, Wiley-VCH, Weinheim, 2003, pp. 59–89.

3 (a) M. J. Burk and R. H. Crabtree, *J. Am. Chem. Soc.*, 1987, **109**, 8025–8032; (b) H. Felkin, T. Fillebeen-Khan, R. Holmes-Smith and Y. Lin, *Tetrahedron Lett.*, 1985, **26**, 1999–2000.

4 (a) M. Gupta, C. Hagen, R. J. Flesher, W. C. Kaska and C. M. Jensen, *Chem. Commun.*, 1996, 2083–2084; (b) M. Gupta, C. Hagen, W. C. Kaska, R. E. Cramer and C. M. Jensen, *J. Am. Chem. Soc.*, 1997, **119**, 840–841; (c) C. M. Jensen, *Chem. Commun.*, 1999, 2443. For reviews, see: (d) D. Morales-Morales and C. M. Jensen, *The Chemistry of Pincer Compounds*, Elsevier, Amsterdam, 2007; (e) *Activation and functionalization of C–H bonds*, ed. K. I. Goldberg and A. S. Goldman, ACS symposium series, American Chemical Society, Washington, DC, 2004, vol. 885; (f) D. Morales-Morales, Iridium-mediated alkane dehydrogenation, in *Iridium complexes in organic synthesis*, ed. L. A. Oro and C. Claver, Wiley-VCH, Weinheim, 1st edn, 2009; (g) D. Bézier and M. Brookhart, Transfer Dehydrogenations of Alkanes and Related Reactions Using Iridium Pincer Complexes, in *C–H Bond Activation and Catalytic Functionalization II*, ed. P. H. Dixneuf and H. Doucet, Topics in organometallic chemistry, Springer, Heidelberg, 2016, vol. 56, p. 189.

5 (a) K. Krogh-Jespersen, M. Czerw, K. Zhu, B. Singh, M. Kanzelberger, N. Darji, P. D. Achord, K. B. Renkema and A. S. Goldman, *J. Am. Chem. Soc.*, 2002, **124**, 10797–10809; (b) K. Zhu, P. D. Achord, X. Zhang, K. Krogh-Jespersen and A. S. Goldman, *J. Am. Chem. Soc.*, 2004, **126**, 13044–13053; (c) S. Kundu, Y. Choliy, G. Zhuo, R. Ahuja, T. J. Emge, R. Warmuth, M. Brookhart, K. Krogh-Jespersen and A. S. Goldman, *Organometallics*, 2009, **28**, 5432–5444; (d) Z. Huang, M. Brookhart, A. S. Goldman, S. Kundu, A. Ray, S. L. Scott and B. C. Vicente, *Adv. Synth. Catal.*, 2009, **351**, 188–206.

6 (a) I. Göttker-Schnetmann, P. S. White and M. Brookhart, *Organometallics*, 2004, **23**, 1766–1776; (b) I. Göttker-Schnetmann, P. White and M. Brookhart, *J. Am. Chem. Soc.*, 2004, **126**, 1804–1811.

7 W. Yao, Y. Zhang, X. Jia and Z. Huang, *Angew. Chem., Int. Ed.*, 2014, **53**, 1390–1394.

8 A. V. Polukeev, R. Gritcenko, K. J. Jonasson and O. F. Wendt, *Polyhedron*, 2014, **84**, 63–66.

9 J. J. Adams, N. Arulsamy and D. M. Roddick, *Organometallics*, 2012, **31**, 1439–1447.

10 (a) X. Zhang, T. J. Emge and A. S. Goldman, *Inorg. Chim. Acta*, 2004, **357**, 3014–3018; (b) R. B. Bedford, M. E. Blake, S. J. Coles, M. B. Hursthouse and P. N. Scully, *Dalton Trans.*, 2003, 2805–2807.

11 G. R. Fulmer, A. J. M. Miller, N. H. Sherden, H. E. Gottlieb, A. Nudelman, B. M. Stoltz, J. E. Bercaw and K. I. Goldberg, *Organometallics*, 2010, **29**, 2176–2179.

12 *Crysalis CCD*, Oxford Diffraction Ltd, Abingdon, Oxfordshire, UK, 2005.

13 *Crysalis RED*, Oxford Diffraction Ltd, Abingdon, Oxfordshire, UK, 2005.

14 G. M. Sheldrick, *Acta Crystallogr., Sect. A: Found. Crystallogr.*, 2008, **64**, 112–122.

15 P. Brulatti, R. J. Gildea, J. A. K. Howard, V. Fattori, M. Cocchi and J. A. G. Williams, *Inorg. Chem.*, 2012, **51**, 3813–3826.

16 D. Martin, D. Moraleda, T. Achard, L. Giordano and G. Buono, *Chem. – Eur. J.*, 2011, **17**, 12729–12740.

17 (a) Y. Xiao, Y. Xu, H.-S. Cheon and J. Chae, *J. Org. Chem.*, 2013, **78**, 5804–5809; (b) J. Chen, T. Yuan, W. Hao and M. Cai, *Catal. Commun.*, 2011, **12**, 1463–1465; (c) R. Paul, M. A. Ali and T. Punniyamurthy, *Synthesis*, 2010, 4268–4272.

18 K. Kunz, U. Scholz and D. Ganzer, *Synlett*, 2003, 2428–2439.

19 (a) D. Olsson, A. Arunachalampillai and O. F. Wendt, *Dalton Trans.*, 2007, 5427–5433; (b) A. Arunachalampillai, D. Olsson and O. F. Wendt, *Dalton Trans.*, 2009, 8626–8630; (c) M. T. Johnson and O. F. Wendt, *Inorg. Chim. Acta*, 2011, **367**, 222–224.

20 K. J. Jonasson, N. Ahlsten and O. F. Wendt, *Inorg. Chim. Acta*, 2011, **379**, 76–80.

21 N. T. Mucha and R. Waterman, *Organometallics*, 2015, **34**, 3865–3872.

22 (a) M. Kanzelberger, B. Singh, M. Czerw, K. Krogh-Jespersen and A. S. Goldman, *J. Am. Chem. Soc.*, 2000, **122**, 11017–11018; (b) A. V. Polukeev, R. Marcos, M. S. G. Ahlquist and O. F. Wendt, *Chem. Sci.*, 2015, **6**, 2060–2067.

23 I. Göttker-Schnetmann and M. Brookhart, *J. Am. Chem. Soc.*, 2004, **126**, 9330–9338.

24 J. Choi, A. H. R. MacArthur, M. Brookhart and A. S. Goldman, *Chem. Rev.*, 2011, **111**, 1761–1779.

25 (a) A. Kumar, T. Zhou, T. J. Emge, O. Mironov, R. J. Saxton, K. Krogh-Jespersen and A. S. Goldman, *J. Am. Chem. Soc.*, 2015, **137**, 9894–9911; (b) A. Brück, D. Gallego, W. Wang, E. Irran, M. Driess and J. F. Hartwig, *Angew. Chem., Int. Ed.*, 2012, **51**, 11478–11482; (c) Z. Huang, P. S. White and M. Brookhart, *Nature*, 2010, **465**, 598–601.

26 A. V. Polukeev and O. F. Wendt, *Organometallics*, 2015, **34**, 4262–4271.